Separation Science and Technology
Publication details, including instructions for authors and subscription information:
http://www.informaworld.com/smpp/title~content=t713708471

Visualization of Flow Fields and Interfacial Phenomena in Liquid-Liquid Solvent Extraction

T. C. Scott[a]
[a] Chemical Technology Division Oak Ridge National Laboratory, Oak Ridge, Tennessee

To cite this Article Scott, T. C.(1987) 'Visualization of Flow Fields and Interfacial Phenomena in Liquid-Liquid Solvent Extraction', Separation Science and Technology, 22: 2, 503 — 511
To link to this Article: DOI: 10.1080/01496398708068966
URL: http://dx.doi.org/10.1080/01496398708068966

SEPARATION SCIENCE AND TECHNOLOGY, 22(2&3), pp. 503-511, 1987

Visualization of Flow Fields and Interfacial Phenomena in Liquid-Liquid Solvent Extraction

T. C. SCOTT

CHEMICAL TECHNOLOGY DIVISION
OAK RIDGE NATIONAL LABORATORY
OAK RIDGE, TENNESSEE 37831

ABSTRACT

Use of a video camera apparatus with a helium-neon laser light source has enabled the detection of flow fields in and around a circulating aqueous droplet which is suspended in a flowing stream of 2-ethyl-1-hexanol. Droplet Reynolds numbers were in the range of 7 to 22. The behavior of the streamlines for flow both inside and outside the droplet was shown to be similar to that predicted for circulating droplets at low Reynolds numbers. Formation of stagnant caps of surfactant at the rear of the droplets was found to suppress the flow patterns inside the droplet and decrease the associated internal fluid velocities.

INTRODUCTION

Contact of droplets of a dispersed liquid phase with a continuous liquid phase represents a basic interaction in liquid-liquid solvent extraction. Mass transfer rates from one phase into the other depend on hydrodynamics of the droplet-continuum system (i.e., velocity profiles around and within the droplet) and physical properties of the transferring chemical species (distribution between the phases, diffusivities of the species, etc.). While properties of chemical species in solution can be investigated apart from the actual mass-transfer system, the flow fields must be evaluated under conditions which are characteristic of the transfer process in question. Complicating the analysis of experimental systems are such phenomena as the formation of stagnant caps on droplets, interfacial movement, boundary layer detachment, and surfactant effects.

It would be extremely useful to be able to observe and quantify such flow fields and complicating phenomena in experimental systems utilizing nonintrusive methods. In many cases a characterization of the types of interactions present could lead to significant improvements in the theoretical treatment of liquid-liquid interfacial mass transfer. The objective of this study is to develop flow visualization techniques which enable the detection and quantization of flow fields which occur in the droplet-continuum, mass-transfer process. A portion of the incident beam from a helium-neon laser is scattered off the interface and off small particulates which are contained in the two liquid phases. Video tapes of the images produced by the scattered light yield detailed pictures of the system. Observations and measurements can be made which describe streamlines for flow of the continuous phase, flow patterns of interfacial movement, and circulation patterns which exist inside droplets.

EXPERIMENTAL APPARATUS

The apparatus used to study flow patterns in the droplet-continuum system consists of three main parts: a flow system which enables suspension of droplets in a continuous stream, a laser which provides the lighting for visualization, and a video camera and recorder which are used to store the images for subsequent playback and analysis. The flow system includes equipment that is necessary to suspend a single droplet of the dispersed phase in an upflowing continuous phase. Droplets are suspended at a fixed position in a tapered glass column (Fig. 1). The droplet is introduced into the column through a hole in the top, while the continuous phase enters at the bottom of the column and exits at the top. Electrodes are located above and below the normal position of the droplet. These are used in studies of the effects of electric fields upon liquid-liquid mass transfer and were not used in collecting the data described in this paper. Figure 2 contains a schematic diagram of the components of the flow apparatus.

The lighting for flow visualization is provided by a 5 mW Melles Griot helium-neon laser (output is at 633 nm). A portion of the incident beam is scattered by the interface and by particulates in the two liquid phases. The beam strikes the droplet normal to, and in the same horizontal plane as, the video camera. Hence, images created by the scattered light yield two-dimensional pictures that are axisymmetric about the spherical coordinate, ϕ (Fig. 3).

The video system is comprised of a Tritronics Model PC5600, high-speed, shuttered, video camera and a Sony Model VO-5800 video recorder. A FOR.A video timer VTG-33 is used to superimpose the date and time onto the video tape (time is indicated to the nearest 0.01 s). A VPA-100 position analyzer allows determination of particle and streamline positions in the video image. Because of the

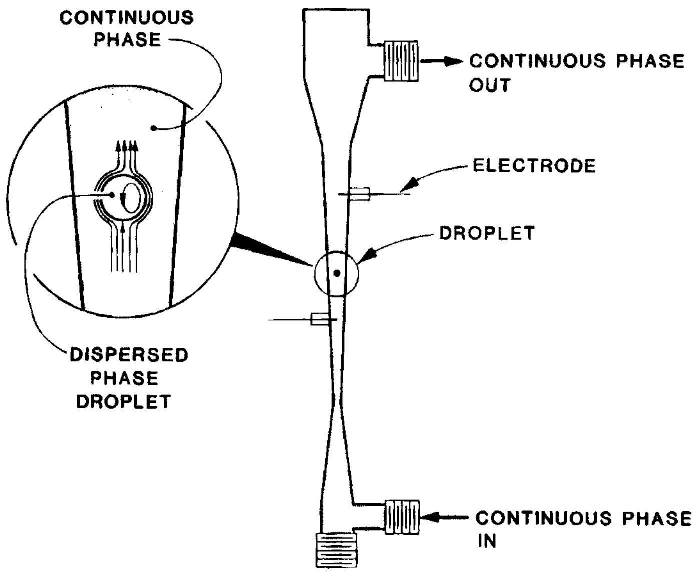

Fig. 1. The experiment centers around a droplet suspended in a flowing continuous phase.

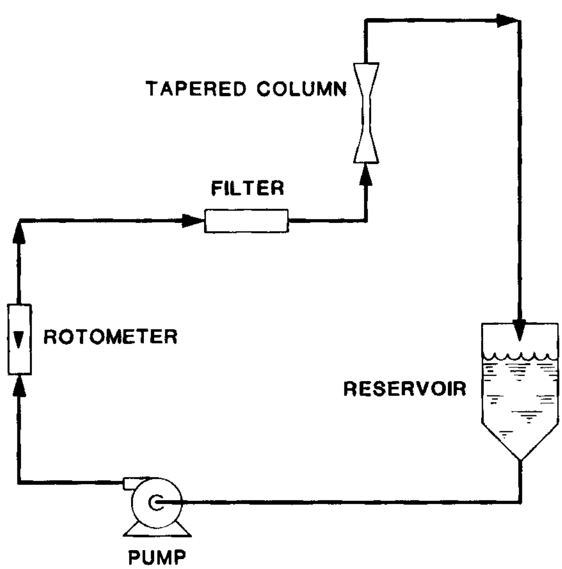

Fig. 2. Schematic diagram of the flow equipment components.

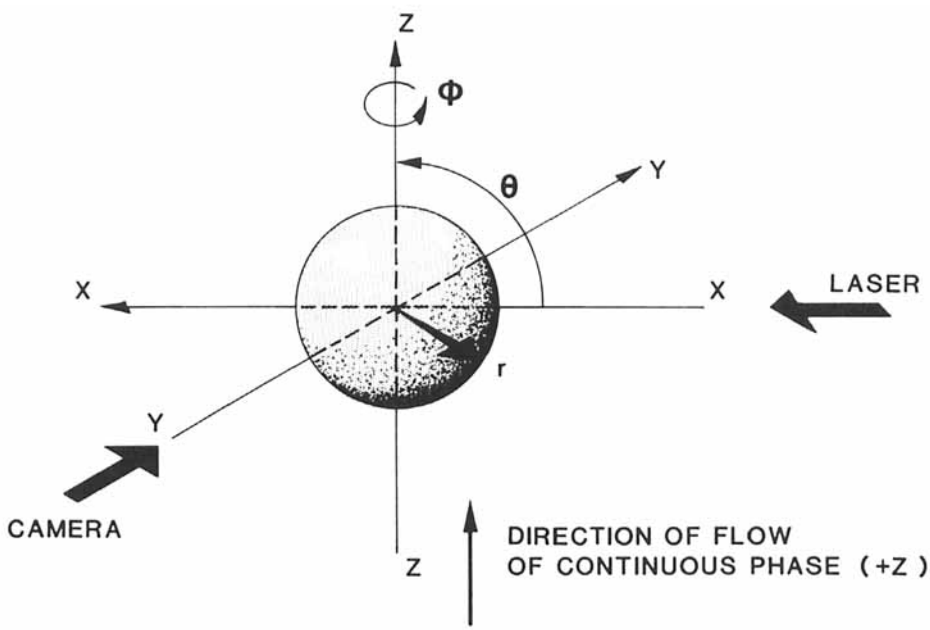

Fig. 3. Internal droplet circulation pattern is independent of the phi (ϕ) coordinate. The positioning of the camera and laser yield circular images located in the XZ plane.

relatively low level of light in the experiments, the video camera was run in an unshuttered mode. This resulted in an equivalent filming speed of approximately 60 frames per second.

An experiment consists of suspending a droplet in the continuous phase such that it is struck by the laser beam and recording the resultant images on video tape for subsequent analysis. In each case, the dispersed phase was water and the continuous phase 2-ethyl-1-hexanol. The length of individual runs varied from 5 min to 2 h, depending upon the purpose. Short runs were designed to examine ideal, circulating droplets, while longer runs investigated behavior during the accumulation of surfactant. In order to facilitate viewing of the streamlines, small amounts of corn pollen (78 μm in diam) were added to the aqueous phase. Corn pollen was chosen on the basis of its size, density, and ability to reflect the incident laser beam.

RESULTS AND DISCUSSION

Qualitative Description of the Flow Patterns in the Droplet-Continuum System

The problem of predicting the mass-transfer characteristics of liquid droplets in a continuous phase has been addressed by a large number of researchers (1-8). In most cases, assumptions had to be made regarding the flow fields present around and within the droplet. If one assumes that the droplet undergoes steady translation with respect to the continuous phase and that the fluid inside the droplet is steadily circulating without turbulence, the streamlines can be calculated for a spherical droplet for flow that takes place either in the low-Reynolds-number, creeping-flow regime (9) or in the high-Reynolds-number, inertial-flow regime (10).

Figure 4 is a schematic diagram of the well known streamlines that occur for the case of a droplet translating in a continuous phase at a low Reynolds number (Re <1). As a consequence of the geometry of the system, flow behavior does not vary in the phi (ϕ) direction. The continuous-phase fluid approaches the droplet with uniform velocity, V_∞. Flow external to the droplet is characterized by streamlines that are curved near the interface and straight at distances relatively far from the interface. Inside the droplet, streamlines form toroidal cells which encircle a stagnation ring. The qualitative description for the case of inertial flow (Re >100) in and around the droplet is similar to that of creeping flow. The behavior of streamlines external to the droplet is much like that which occurs in the case of creeping flow, and toroidal flow cells are found to exist within the droplet. The main differences are found in the shapes of the toroidal cells and in the associated velocity gradients inside the droplet.

Video tapes of the aqueous droplet suspended in the upflowing 2-ethyl-hexanol have been analyzed to assess the qualitative nature of the flow fields. Figure 5 is a photograph of a single frame of a flow-visualization experiment obtained using the aforementioned apparatus and techniques. It is immediately obvious that the flow patterns observed in the experimental system are very similar to the patterns predicted by theory (see Fig. 4). However, some distinct differences in flow patterns exist that are not easily discernible utilizing still photography.

A review of the video tape reveals that, in fact, there is a small translation of the toroidal cells about the phi (ϕ) axis and that particulates tend to spiral around from one flow cell to another. This slight instability occurs because the droplet is slowly rotating in the theta (θ) direction (Fig. 3). This slow rotation occurs because the streamlines of the continuous phase are not exactly aligned with the gravitational field of the earth. Attempts to completely stop this rotation have not been successful; however, the rotational velocity can be reduced to <2% of the external fluid velocity.

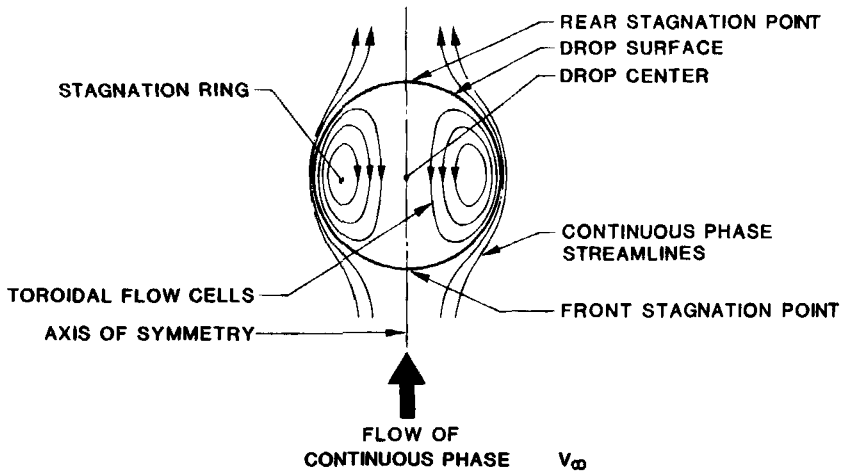

Fig. 4. Schematic diagram of Hadamard flow cells in a droplet.

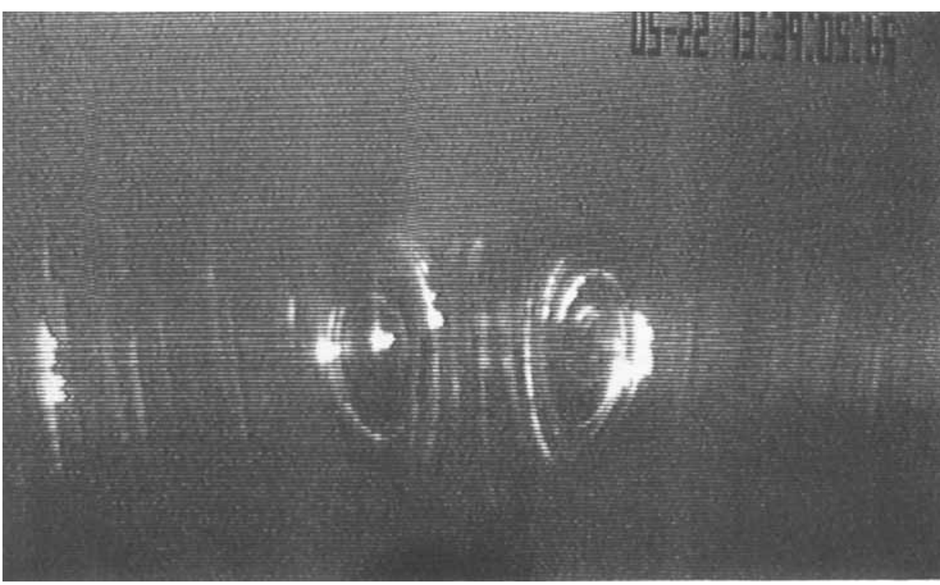

Fig. 5. Hadamard-type streamlines in suspended aqueous droplet.

TABLE 1
Data for the flow-visualization experiments

Run No.	Droplet radius (cm)	Suspension velocity (cm/s)	Reynolds No.[a]
1	0.133	8.43	22
2	0.116	6.20	14
3	0.094	3.88	7
4	0.092	3.95	7

[a]$Re = (2\ R\rho V_\infty)/\mu$, where ρ and μ are the density (0.83 g/cm^3) and viscosity (8.65 cP) of 2-ethyl-1-hexanol, respectively, R is the droplet radius, and V_∞ is the suspension velocity of the droplet.

The position analyzer and timer were used to determine the suspension velocity and Reynolds numbers for several different droplets. Table 1 lists the size, external fluid velocity, and Reynolds number for each of the droplets studied.

The range of experimental droplet sizes is restricted by the apparatus. Droplets significantly larger than 5 mm in diameter are subject to appreciable wall effects in the column, and those significantly smaller than 1 mm in diameter cannot be accurately observed, utilizing the current lenses. The suspension velocity was determined by measuring the position of particles in the continuous phase as a function of time. This velocity was determined on streamlines located in areas free from effects due to the droplet or the wall of the column. The Reynolds numbers of the droplets are in the range of 7 to 22; hence, the behavior of internal circulation patterns would be expected to be intermediate between that predicted for creeping flow and for inertial flow. A quantization of the geometry and velocity of the internal flow cells will be treated in a future publication.

INTERFACIAL EFFECTS: FORMATION OF STAGNANT CAPS ON DROPLETS

The addition of corn pollen into the system also introduced minute dust particulates, as well as small amounts of unspecified surfactants. Hence, droplets allowed to remain in the column for (>10 min) were observed to accumulate surfactant at the interface. When the droplet is suspended, surfactant contained in the continuous phase impinges upon the droplet at the front stagnation point and is swept backward to the rear stagnation point. As more of the surfactant contacts the droplet, a spherical cap forms about the rear. This cap may grow to cover a significant portion of the surface area of the droplet.

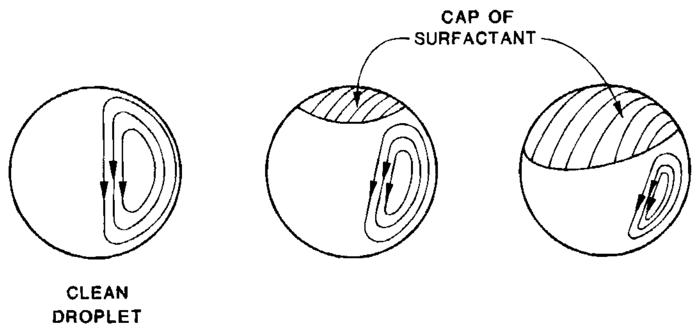

Fig. 6. Effect of the formation of a stagnant cap of surfactant upon internal flow patterns.

As the stagnant cap grows larger, internal circulation patterns are affected. Figure 6 contains a schematic diagram that describes the characteristics of internal flow patterns under the influence of surfactant accumulation. The size and velocity of the toroidal flow cells decrease as the size of the cap increases. Circulation is almost nonexistent in the portion of the droplet enclosed by the cap, as illustrated by the extremely slow velocity of pollen particles observed in this region. These observations agree with those of Horton (11) who studied single-droplet phenomena using high-speed motion pictures and still photography.

CONCLUSIONS

Visualization of flow fields in a liquid-liquid, droplet-continuum system has been accomplished utilizing a video camera apparatus with a helium-neon laser as the lighting source. Video tapes of droplets yield detailed pictures of internal droplet mixing, continuous-phase streamlines, and stagnant cap formation at the interface.

Flow-visualization results similar to those cited in this paper have been discussed by other investigators; however, in previous studies visualization was accomplished by using high-speed movie cameras or by still photography. It was difficult or impossible to view the phenomena as they were taking place. After each experiment was completed, the film had to be developed and then projected onto a screen containing grid markings in order to obtain quantitative measurements. The apparatus used in this study offers several advantages over previous methods: (1) the capability for monitoring experiments in progress, (2) the immediate analysis of results, and (3) increased accuracy in the quantitative measurements (e.g., velocity measurements). Use of this apparatus in the study of liquid-liquid, interfacial, mass transfer should augment the ability of researchers to model hydrodynamics of such systems.

ACKNOWLEDGMENTS

This research was sponsored by the Office of Basic Energy Sciences, U.S. Department of Energy under Contract No. DE-AC05-84OR21400 with Martin Marietta Energy Systems, Inc.

REFERENCES

1. Brignell, A. S., Int. J. Heat Mass Transfer 18, 61 (1975).

2. Jones, L. E., Jr. and R. B. Beckmann, J. Fluid Mech. 32, 376 (1968).

3. Kronig, R. and J. C. Brink, Appl. Sci. Res. A2, 142 (1951).

4. Ruckenstein, E., Int. J. Heat Mass Transfer 10, 1785 (1967).

5. Brunson, R. J. and R. M. Wellek, AIChE J. 17, 1123 (1971).

6. Handlos, A. E. and T. Baron, AIChE J. 3, 127 (1957).

7. Rose, P. M. and R. C. Kintner, AIChE J. 12, 530 (1966).

8. Angelo, J. B., E. N. Lightfoot, and D. W. Howard, AIChE J. 12, 751 (1966).

9. Hadamard, J., C. R. Hebd. Seanc. Acsd. Sci. Paris 152, 1735 (1911).

10. Harper, J. F. and D. W. Moore, J. Fluid Mech. 32, 367 (1968).

11. Horton, T. J., T. R. Fritsch, and R. C. Kintner, Can. J. Chem. Engr. 43, 143 (1965).